THE ASTROPHYSICAL JOURNAL, 288:142–147, 1985 January 1

STRUCTURE AND ORIGIN OF VELOCITY FLUCTUATIONS IN THE H II REGION SHARPLESS 142

JEAN-RENÉ ROY
Département de physique, Observatoire astronomique du mont Mégantic, Université Laval
AND
GILLES JONCAS
Observatoire de Marseille
Received 1984 June 25; accepted 1984 July 23

ABSTRACT

Close to 41,000 Hα radial velocities have been measured across most of the evolved H II region S142 ($\theta \approx 25'$), allowing a systematic study of velocity fluctuations. Using grids of different mesh size to subdivide the H II region, the mean velocity dispersion, σ, is found to be dependent on mesh size L. A well-defined correlation in the form of a power law $\sigma \approx L^{0.30}$ is found. Because of the ambiguous interpretation of this result in terms of turbulence, the *structure function*, B, which tests for velocity correlation at all scales has also been calculated. The structure function does not approach zero for 3″(0.1 pc) $< r <$ 90″(1.6 pc). A linear relation $B \approx r$, i.e., $\Delta V(r) \approx r^{0.50}$ is found for 90″(1.6 pc) $< r <$ 500″(9 pc); on larger scales, decorrelation occurs. A brief qualitative analysis is attempted in terms of a turbulent energy cascade in a supersonic and compressible fluid. Kelvin-Helmholtz instabilities are suggested for the generation and maintenance of nebular turbulence.

Subject headings: nebulae: H II regions — nebulae: individual — turbulence

I. INTRODUCTION

The study of velocity dispersion in the interstellar medium has proven to be a useful tool for the evaluation of the roles played by gravitation, gasdynamical processes, and turbulence in inducing motions in the interstellar medium. For H II regions and molecular clouds, the velocity width $\sigma(\Delta V)$, in excess of thermal motions and natural width, inferred from the line width ΔV has been used to relate with other physical or galaxian parameters. Many observations of the velocity width of radio and optical spectral lines of interstellar clouds have been stimulated by its potential use in solving fundamental problems. Let us mention the use of velocity dispersion of giant extragalactic H II regions as an extragalactic distance calibrator (Melnick 1977, 1978; de Vaucouleurs 1979) or of the velocity widths of molecular cloud spectral lines for the exploration of the nature of interstellar turbulence (Larson 1981; Leung, Kutner, and Mead 1982; Myers 1983). Optical astronomers have used two approaches for the measurement of nebular spectral lines. The more traditional one is based on large-aperture Fabry-Pérot (F-P) scans. (See Arsenault and Roy 1984 and references therein). The other has been stimulated by the recent arrival of efficient panoramic detectors that has encouraged the use of echelle spectrographs which give equivalent spectral resolution with the advantage of spatial resolution along the slit (e.g., Gallagher and Hunter 1983; Rosa and Solf 1983). Both methods derive the nonthermal component of the line width by deconvolving the observed profile with the instrumental and the thermal profiles. An important limitation in deriving the velocity width of line profiles is the large uncertainty of the thermal broadening, because of a poor knowledge of nebular temperature. This problem is particularly severe for extragalactic H II regions where temperatures can deviate by a large amount from the canonical value of 10^4 K (e.g., Rayo, Peimbert, and Torres-Peimbert 1982).

Line broadening in excess of thermal motions may be related to disordered or turbulent velocity fields. Therefore, it is important to determine if this disordered velocity field, measured by the velocity width of spectral lines, scales with the size of clouds in the interstellar medium (Larson 1979, 1981). In comparison with molecular clouds, ionized regions have received little attention from this point of view, if we except the controversial relation found for giant extragalactic H II regions (Melnick 1977; Gallagher and Hunter 1983). Because the coulomb mean free path in a fully ionized nebula is short, viscous stresses are small and momentum transport is mostly due to bulk motion (Lazareff 1983). Therefore H II regions are likely to have very high Reynolds numbers (Kaplan and Pikelner 1970).

In this paper, we use detailed Hα velocity maps of H II region Sharpless 142 to present two approaches for the determination of velocity dispersion in H II regions in an attempt to establish the presence and possibly the characteristics of nebular turbulence. Instead of using the line width of a spectral line profile, we measure the velocity dispersion $\sigma(V)$ associated with the variation of radial velocity V across the nebula. In a second step, we take advantage of the stochastic nature of turbulence to compute the *structure function*, a statistical function which tests for correlation. This method was used for the first time by Von Hoerner (1951). Since then it has been applied by Courtès (1955), by Münch (1958) who used Wilson *et al.*'s (1959) abundant data on M42 and by Louise and Monnet (1970). The method was recently rediscussed in detail and applied to a set of molecular cloud radial velocities by Scalo (1984).

A crucial advantage of radial velocities is that they do not require a knowledge of temperature. A major inconvenience is that a huge number of accurate measurements is required to lead to a statistically significant result. Fortunately modern spectroscopic techniques, efficient panoramic detectors, and image processing greatly alleviate this shortcoming.

II. FABRY-PEROT INTERFEROMETRY OF S142

S142 is a relatively large ($\theta \approx 25'$) and evolved H II region located in the Perseus arm ($l = 107.14, b = -0.96$) at ~ 3.5 kpc from the Sun (Moffat 1971; Humphreys 1978). A small molecular cloud of 200 $M_\odot$ (^{12}CO $V_{LSR} = -41.0$ km s^{-1}) has been observed by Israël (1980) east of the H II region which is ionization bounded on that side. Four closely linked clouds of neutral hydrogen (total mass of 5800 $M_\odot$) are located east, south, and in front of S142 (Joncas *et al.* 1984). The gas complex appears to be seen almost edge on. An open cluster, NGC 7380, is associated with the nebula and has been investigated by Moffat (1971). The O6 star DH Cep (HD 215835), a spectroscopic binary and a member of NGC 7380, is the main source of ionization. It is located in the low-brightness western section of the H II region which is density bounded on that side. The 21 cm continuum radio map shows that the mean electron density is about 20 cm^{-3} and decreases east to west. More details and references to other works can be found in Joncas and Roy (1984*b*).

Thirteen Hα interferograms were obtained with a $f/0.95$ F-P camera attached to the 1.60 m telescope of the Observatoire astronomique du mont Mégantic. A complete description of the instrumentation and of the reduction procedures to obtain radial velocity maps from digitized F-P interferograms is given in Joncas and Roy (1984*a*, *b*). A tunable and servo-stabilized F-P interferometer having a free spectral range of 283 km s^{-1} was used. The FWHM of the instrumental profile is 20 km s^{-1}, resulting in an effective finesse of 14 at Hα, or a mean linear dispersion of 1.7 nm mm^{-1} on the detector (IIIa-F plate). A total of 40,983 radial velocities were measured over S142, with a spatial resolution reaching 3″. The histogram of the velocities is very close to a normal distribution; the mean LSR velocity is -35.6 ± 0.1 km s^{-1} with a dispersion $\sigma = 12.5 \pm 0.1$ km s^{-1}. The radial velocity maps show the presence of a velocity gradient across the nebula of 1 km s^{-1} per projected parsec. Terminal velocities of up to 35 km s^{-1} are measured in the western and southwestern part of the nebula. These observations are in agreement with the predictions of the champagne model of Tenorio-Tagle (1979).

III. THE MEASUREMENT OF VELOCITY FLUCTUATIONS IN S142

a) The Dispersion of LSR Velocities

i) *The Results*

This large number of radial velocity points allows one to study the variation of V across S142. In order to do this, we have subdivided the surface of the H II region into grids with different mesh size. The smallest mesh size (15″) was chosen to ensure that a sufficient number of velocity points would be present in each window; the other window sizes were chosen at 30″, 45″, 60″, 90″, 120″, 150″, and 180″ (60″ $\approx$ 1.1 pc on the nebula). The largest window was set to be smaller than the scale at which large scale motions dominate the kinematics of S142. Maps of the velocity dispersion corresponding to the 60″ grid can be found in Joncas and Roy (1984*b*). We have called velocity dispersion the standard deviation from the mean velocity measured in each window, whenever more than 10 radial velocities had been measured. Figure 1 presents the histograms of velocity dispersion for the grids with the 15″ and 150″ mesh sizes. Table 1 summarizes the data on the velocity dispersion for the various sampling grids. Values of the mean dispersion $\bar{\sigma}(V)$, of the most probable value of dispersion $\sigma(V)$, of the standard deviation s, and of the skewness S_k for the histograms corresponding to each mesh size L are given. Because the different areas have not been sampled equally, not all 40,983 velocities were used in calculating the dispersions. In the last column of Table 1, N indicates the number of windows over the nebula, each having more than 10 measured radial velocities. With increasing L, N diminishes but the number of points within each window increases. A well-defined correlation between $\sigma(V)$, the most probable value of dispersion, and

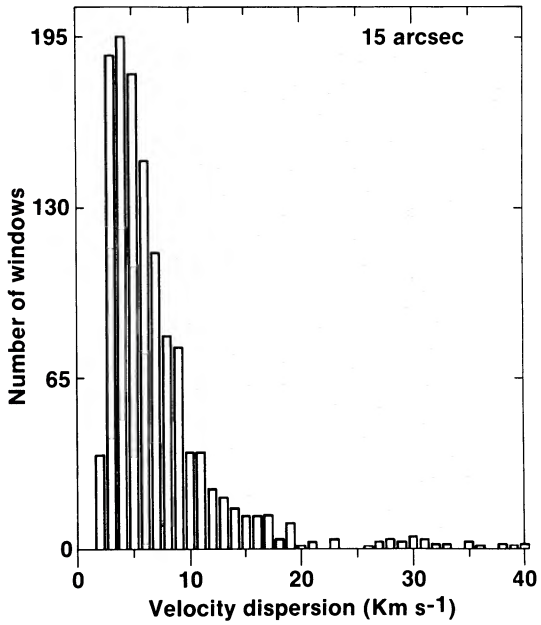

FIG. 1*a*

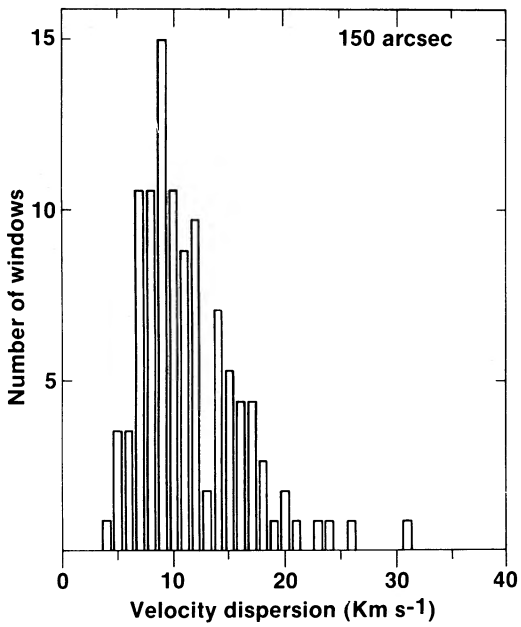

FIG. 1*b*

FIG. 1.—Histograms of velocity dispersions from the mean V_{LSR} in each window of the 15″ and 150″ mesh size sampling grids of S142. See Table 1.

TABLE 1

VELOCITY DISPERSION FOR DIFFERENT MESH SIZE FOR H II REGION S142

L (arcsec)	$\bar{\sigma}(V)$ (km s^{-1})	$\sigma(V)$ (km s^{-1})	S_k	s (km s^{-1})	N
15.....	7.2	4.0 ± 0.2	2.2	5.6 ± 0.1	1247
30.....	8.5	6.0 ± 0.1	1.6	5.4 ± 0.1	1632
45.....	9.2	6.0 ± 0.2	1.4	5.6 ± 0.1	987
60.....	9.8	7.0 ± 0.2	1.4	5.6 ± 0.2	643
90.....	10.6	7.0 ± 0.3	1.2	5.3 ± 0.2	302
120.....	10.8	8.0 ± 0.4	1.0	5.2 ± 0.3	192
150.....	11.4	9.0 ± 0.4	0.5	4.8 ± 0.3	120
180.....	11.4	9.0 ± 0.5	0.3	4.6 ± 0.4	88

the mesh size is seen. Figure 2 shows this relation where L has been converted to l (pc) assuming a distance of 3.5 kpc for S142. A least squares fit for the power law $\sigma(V) \approx al^n$ gives $a = 6.46$ and $n = 0.30 \pm 0.02$. The point at $l = 27$ pc corresponds to the e-folding width (17.7 km s^{-1}) of the histogram of the 40,983 velocities measured over the whole nebula; the e-folding width of the velocity profile of a spectral line corresponds to the most probable velocity of gas motions provided the motions have a Maxwellian distribution. The correlation coefficient $r = 0.99$ implies a highly significant correlation. The increasing skewness (S_k) with decreasing mesh size (L) may originate in part from the fact that although the main distribution shifts to smaller values of velocity dispersion, the highest dispersions (20–35 km s^{-1}) remain present what ever the mesh size.

ii) *Interpretation*

It is important to understand what the measured velocity dispersions physically mean when deduced from Hα radial velocities. Fluctuations of radial velocities observed across a nebula could be produced by nonuniform dust absorption which would affect the depth of line of sight over which the velocity field is sampled. The importance of this effect in S142 is probably negligible: maps of velocity dispersion of this H II region (Joncas 1983; Joncas and Roy 1984*b*) show no systematic trends of velocity dispersion across the nebula. The optical thickness of S142 is likely to be small enough, so that the nebula can be treated as transparent at Hα. Thus each separate radial velocity gives an emissivity-weighted value for the features of different velocities encountered over various depths in the line of sight. With increasing separation between the lines of sight, one expects to see structures further apart and, therefore, more different in velocities. However, the probability of sampling different "streams" throughout a transparent nebula remains the same for all lines of sight if they have all the same length through the nebula. Looking through each window of the grid corresponds to sampling the velocities in a given volume of the nebula; changing the mesh size and keeping it small with respect to the H II region diameter changes the volume but not its depth. With increasing mesh size, we keep recognizing the same basic structures from one grid to another. Consequently, the $\sigma(V) - L$ relation reflects a correlation between size and velocity fluctuation. Because the dispersion is measured for all the velocities in each window without regards to scale, there is smearing for all scales smaller than the mesh size considered. Since the number of velocities over each window increases as the square of the mesh size, the larger mesh sizes are more heavily weighted by small-scale velocities. This produces a smoother slope of the $\sigma(V) - L$ relation than if velocity dispersions were related to discrete scales.

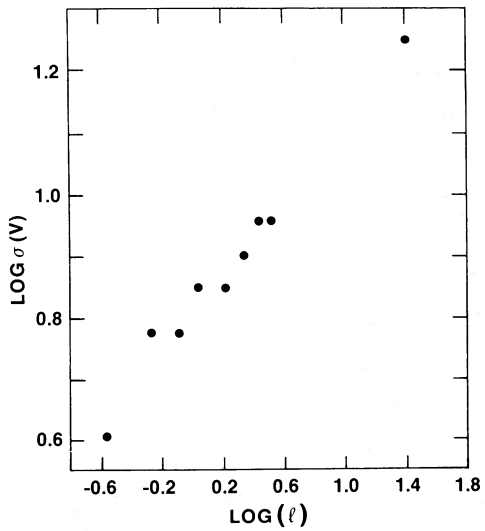

FIG. 2.—Log-log plot of the velocity dispersion as a function of mesh size on the nebula. The width of each window on S142 has been converted into parsecs using an assumed distance of 3.5 kpc.

We can establish similarities between our observations of $\sigma(V)$ and the velocity width deduced from line profiles. Each radial velocity point measured on the nebula is the central velocity of a line profile contained in the width of a 3″ fragment on a F-P interference fringe. For example, the mean radial velocity obtained from a 1′ window should be equal to the one measured with a F-P spectrophotometer having a 1′ diaphragm centered at the position of the above window if the former mean is obtained after weighting for its particular intensity. Consequently, the calculated standard deviation or dispersion with respect to the mean radial velocity should be a measure of the excess velocity width of the corresponding profile assuming the absence of large temperature fluctuations on a scale smaller than the window size. To substantiate this hypothesis, we have compared radio line observations by Garay and Rodríguez (1983) [H125α] and Pedlar (1980) [H166α] with our dispersion velocities. The former used a 10′ HPBW and obtained a "turbulent" velocity of 11 ± 1 km s^{-1} (e-folding width). For a similar mesh size we calculate from Figure 2 a 12.0 ± 0.6 km s^{-1} most probable velocity dispersion. Pedlar (1980) used a 36′ HPBW thus supposedly encompassing the whole nebula. His velocity width in excess of thermal motions is 12.4 km s^{-1}, at odds with our value of 17.7 ± 0.1 km s^{-1} taken from all our radial velocity points. This can be explained if the antenna was not pointed at the center of the nebula but favored its brightest part thus preventing the nebula from filling the antenna lobe. This appears to be the case when we compare the LSR velocity derived from the radio profiles: −37.2 km s^{-1} for Garay and Rodríguez and −43.3 km s^{-1} for Pedlar. The more negative velocities (Joncas and Roy 1984*b*) are found near the molecular cloud where S142 is the brightest at Hα. Despite this discrepancy with Pedlar's result, we feel that there is a close relation between line profile observations and the histogram of Hα radial velocities even though the latter is not weighted for emissivity. However, we cannot certify that the agreement would hold at the small mesh sizes. If indeed we are measuring an excess velocity width, it is far from certain that this excess is a measure of turbulence. Scalo (1984) describes several ways which can induce line profile broadening; for example, the observed power-law rela-

tion between scale and velocity dispersion may simply result from the sampling of a larger number of velocity fluctuations with increasing mesh size. We must also bear in mind the expansion of the nebula; its effect was not subtracted from the velocity field. Geometrical effects may also produce line broadening even in the absence of spherically symmetric expansion or collapse. The next method avoids many of these pitfalls; in particular, the velocity gradient will be filtered out.

b) *The Structure Function*

i) *The Calculation*

If an H II region is turbulent, a fundamental property is spatial fluctuation in density and velocity. A method available to astronomers for the study of fluctuations in the ISM is the correlation method (Kaplan 1966; Kaplan and Pikelner 1970). The correlation function, is $D(r) = v(r')\,v(r'')$, and the structure function is $B(r) = [v(r') - v(r'')]^2$, where $r = r' - r''$ and $v(r')$ and $v(r'')$ are the measured radial velocities at points r' and r'', and r is the scale under investigation for velocity correlation. However, these functions can only be used under certain conditions: (1) the turbulence has to be homogeneous and isotropic; and (2) the fluid must be free of motion discontinuities and of large-scale trends. Scalo (1984) has shown the structure function to be more suitable for the study of fluctuations in interstellar clouds.

The first restriction requires that the velocity field be independent of position and direction. S142 experiences a champagne flow which excludes the desired independency. However, the extensive data coverage ensures a quantitative description of the velocity gradient; thus the large-scale velocity trends were easily removed. Nevertheless, we remain uncertain about the presence of small-scale velocity structures that could destroy the homogeneity of stochastic fluctuations. In any event, the structure function, $B(r)$, requires the turbulence to be only locally homogeneous and isotropic (Scalo 1984); therefore, the structure function has in this a clear practical advantage over the correlation function. The second restriction can be discarded. Our observations of S142 do not reveal any obvious velocity discontinuities. Finally, H II regions are gaseous, therefore compressible; a precise theory of turbulence for compressible fluid does not exist. Despite the smearing effect caused by the averages along the line of sight of the observed velocities (Scalo 1984), the correlation method can still be used to give an idea of the global behavior of turbulence, especially, if we have at our disposal a large sample of velocity points with a good resolution (accuracy of measurement $\lesssim 0.1[B(r)]^{1/2}$, i.e., ± 2 km s^{-1}).

Table 2 gives the results of our calculation of the structure function; r is the separation between the velocity points, $B(r)$ is the structure function, $\Delta B(r)$ is the statistical uncertainty, and N is the number of velocity points having separation r. The relation between B and r is shown in Figure 3. To bring out the different features, this relation is drawn on linear and logarithmic scales. Three different correlation ranges can be seen. From 6″ (0.1 pc) to 75″ (1.4 pc), we almost have a scatter diagram; from 90″ (1.6 pc) to approximately 500″ (9 pc), we have a well-defined relation; from 500″ (9 pc) onward, $B(r)$ becomes incoherent. Decorrelation may come from the fact that $B(r)$ looses its meaning when the separation r is larger than a certain fraction of the diameter of the object. A similar behavior is present in the ρ Oph molecular cloud (Scalo 1984). For both objects the transition occurs when r is of the order of the cloud radius. This may set an upper limit to the dimensions of large-scale velocity fluctuations. Even if the statistical uncertainty on $B(r)$ becomes larger than 5% for separations larger than 500″ (9 pc), its effect is not large enough to destroy the correlation. There is a simple test to verify if the large-scale velocity gradient in S142 was well substracted from the velocity field used to calculate the structure function. If one expands the equation for $B(r)$, the structure function becomes a constant equal to twice the mean velocity fluctuation squared in the absence of correlation. Using points (Fig. 3*a*) with a statistical uncertainty $\lesssim 5\%$, we can put a limit of roughly 320 km^2 s^{-2} for $B(r)$. This value is about twice the variance of all our radial velocity points as expected.

TABLE 2

THE STRUCTURE FUNCTION FOR DIFFERENT VALUES OF SEPARATION BETWEEN RADIAL VELOCITY POINTS

r (arcsec)	B (km^2 s^{-2})	ΔB (km^2 s^{-2})	N
3.....	55	2	5961
6.....	100	3	3905
9.....	117	4	3525
15.....	110	3	6873
21.....	135	4	2036
30.....	125	3	5114
39.....	123	5	1160
45.....	129	4	3846
51.....	136	8	512
60.....	128	3	5535
75.....	125	4	3493
90.....	158	6	1981
120.....	159	5	2963
150.....	170	6	1362
180.....	186	6	2197
210.....	179	8	1099
240.....	209	7	1780
270.....	228	11	928
300.....	238	10	1469
330.....	283	17	688
360.....	287	12	1211
420.....	295	16	925
480.....	320	21	751
510.....	303	25	440
540.....	368	24	563
555.....	333	29	486
585.....	337	60	133
600.....	361	22	466
615.....	275	31	385
630.....	227	20	310
660.....	224	27	459
720.....	154	36	178

ii) *Interpretation*

Since the coordinates of the radial velocity points are known to $\pm 3''$, little weight should be given to the point at 3″ (0.05 pc) in Figure 3. $B(r)$ does not approach zero at small separations ($r \lesssim 75''$). Possibly by coincidence, velocity fluctuations are very close to the sound velocity. Smearing by projection effects in two dimensions (Scalo 1984) lessens the ratio of "observed" velocity dispersion to true dispersion as one goes to smaller scales; for $r \leq 75''$, the "observed" dispersions may become of the same order or smaller than the errors of the radial velocity measurements. However, it is difficult to verify this hypothesis. Moreover, it is puzzling that the transition between noise and presence (discussed next) of correlation takes place rather suddenly at the sound velocity. Maybe there is no subsonic turbulence in S142.

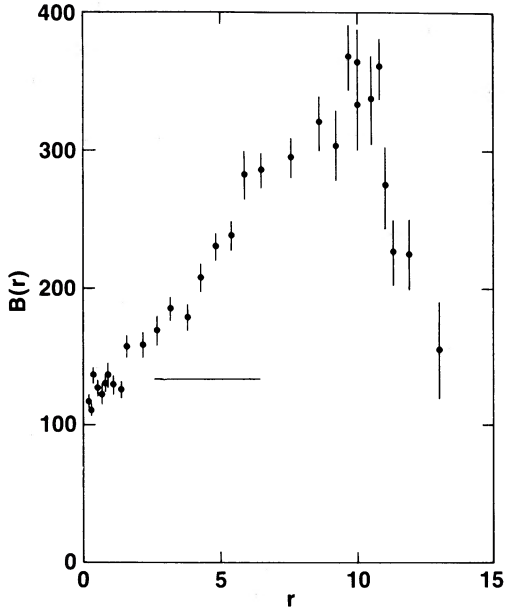

FIG. 3*a*

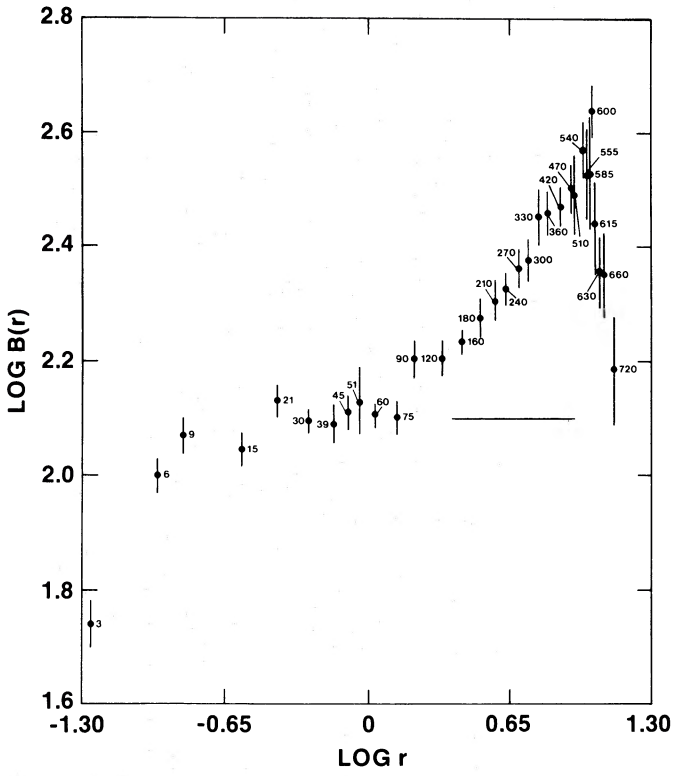

FIG. 3*b*

FIG. 3.—(*a*) Plot of the structure function, B, as a function of separation, r, between radial velocity points. The vertical bars correspond to the statistical uncertainty of the calculated points. The horizontal bar indicates the sound velocity in S142. (*b*) Log-log plot of the structure function as a function of the separation between radial velocity points. The vertical and horizontal bars have the same signification as above. The small figures indicate scale in arcsec. Units of r are in parsecs in (*a*) and (*b*).

For 90″ (1.6 pc) $\leq r \leq$ 500″ (9 pc), the structure function takes the form $B \approx r$, i.e., $\Delta V \approx r^{1/2}$. A turbulent energy cascade (Kolmogorov 1941) is a reasonable interpretation of the observed slope. Consequently, if we interpret the velocity fluctuations described by the structure function as disordered motion, turbulence is mainly supersonic in S142. As a reference, Kolmogorov's law of dissipationless energy cascade for incompressible and subsonic turbulent flows is described by $B \approx r^{2/3}$, i.e., $\Delta V \approx r^{1/3}$. Not surprisingly, the relation for S142 is different from Kolmogorov's law; the observed fluid is compressible and the motion supersonic. The chief influence of compressibility is that the fluid is constantly radiating energy in the form of sound waves which eventually transform into heat (Lighthill 1955). However, as remarked to us by J. M. Scalo, this is true only for compressibilities $\delta\rho/\rho \ll 1$. Otherwise, Lighthill's theory is not valid. Even though the sound waves apply at very small $\delta\rho/\rho$, compressibility acts as a dissipation mechanism responsible in part for the steeper spectral slope. In addition, energy dissipation will likely be enhanced in supersonic turbulent flows. Energy is dissipated on large scales by shock fronts, thus leaving less energy for small cells. Therefore, if a nebula is turbulent, its energy cascade will be steeper than predicted by Kolmogorov's law.

IV. DISCUSSION

What is the origin of turbulence in S142 and how is it maintained? Turbulence is a strongly damped stochastic system with viscous losses being in general the main energy drain. In order to survive, turbulence needs a constant energy supply. Common sources of energy for turbulent velocity fluctuations are shear in the mean flow and buoyancy (Tennekes and Lumley 1972). Buoyancy is generated by density fluctuations. Such fluctuations would be short lived in a champagne flow because of the pressure gradient and of the expansion of the nebula which contribute to the destruction of density inhomogeneities. On the other hand, the jetlike emergence of the ionized gas due to the champagne flow suggests the presence of Kelvin-Helmhotz instabilities (Blake 1972; Norman *et al.* 1982).

These instabilities could develop over the sides of the champagne flow and then be driven by the flow of the shocked intercloud medium; the waves would arise toward the front and propagate back along the interface with the H II region. Once the waves have grown sufficiently, there will be a shearing of the wave leading to vorticity and a growing boundary of turbulent eddies. Intense smaller scale turbulence is generated between the vortices, leading to a turbulent cascade process. Blake (1972) gives relations from which the growth time and the growth speed of the waves can be calculated in the absence of a magnetic field. The e-folding growth time, $t_{\text{K-H}}$, of the Kelvin-Helmhotz instability waves is

$$t_{\text{K-H}} = \left[\frac{k^2 \rho_1 \rho_2 v^2 \cos^2\theta \cos^2\varphi}{(\rho_1 + \rho_2)^2} + \left(\frac{\rho_2 - \rho_1}{\rho_2 + \rho_1} \right) gk \cos\theta \right]^{-1/2}$$

and the growth speed, $v_\perp$, of the waves into the flow in the linear regime is given by

$$v_\perp = \left[\frac{\rho_1 \rho_2}{(\rho_1 + \rho_2)^2} v^2 \cos^2\theta \cos^2\varphi \right]^{1/2},$$

where ρ_1 and ρ_2 are, respectively, the densities of the intercloud medium and H II region; v is the velocity of the champagne flow; φ is the half–cone angle of the champagne flow and θ is the angle between the normal to the surface of the ionized gas flow and the normal to the cone axis; g is the acceleration of the flow and k is the wavenumber of the largest instability. Assuming mean densities of 20 cm^{-3} and 1 cm^{-3} for S142 and the intercloud medium, an average speed of 15 km s^{-1} for the flow, a half–cone angle of 45° and a maximum wavelength of 8 pc (Fig. 3), the instability needs *less than* 10^6 yr to grow. The unstable waves grow in amplitude at a speed of approximately 6 km s^{-1}. These values imply that the nebula is completely turbulent in a maximum of 10^6 yr. Since S142 is 2–3 × 10^6 yr old (Moffat 1971), the Kelvin-Helmholtz instability may provide a driving mechanism. Finally, we can add that the vortices created by the nonlinear growth of the Kelvin-Helmholtz instabilities have eddy speeds proportional to the mean axial velocity of the flow (Henriksen, Bridle, and Chan 1982) and would be 15 km s^{-1} for S142. Other sources of energy acting at various scales in an H II region are likely to give rise or to sustain turbulence generated by the Kelvin-Helmholtz instabilities. Let us mention, for example, jet generation by radiation-driven ionization fronts interacting with a nonuniform neutral cloud edge (Sanford, Whitaker, and Klein 1982), wakes from stellar wind bubbles (Kahn 1980), and explosive disruption at the H II–H I interface.

Turbulence is a complex phenomenon and its study in the interstellar medium does not make its understanding any easier. In a recent review, Cantwell (1981) criticizes the Eulerian spatial correlation approach, used in this paper, for the study of turbulent fluids. This approach does not offer any information about how the moving large eddies are laced together to complete the flow field. This is apparent from the incoherent behavior of the structure function at large separation. Laboratory studies cannot tell us how the coupling is made between large and small scale eddies.

The behavior of turbulence is highly dependent on the presence of perturbations during its transition phase (Cantwell 1981), which suggests that the structure function would be different from one object to the other. It may thus be possible, by calculating the structure function of H II regions having different geometries, age, exciting stars (for stellar wind effects), and, more explicitly, *not* experiencing a champagne flow to detect the presence and relative importance of different sources of mechanical energy.

V. SUMMARY

We have used Hα radial velocities measured at nearly 41,000 positions across the evolved H II region S142 to study the fluctuations of radial velocities and to investigate possible clues on the nature of turbulence in S142. The main results of our study are as follows:

1. The calculation of standard deviations from a large amount of radial velocity measurements indicates a relation ship between velocity dispersion and scale of the form $\sigma \approx L^{0.30}$. However, smearing effects due to sampling makes it difficult to interpret this relation in terms of turbulence.

2. The computation of the structure function yields valuable indication on the behavior of turbulence in S142. The H II region S142 appears to experience supersonic turbulence. The turbulent cascade has a steep spectral slope which could be explained in part by the compressible nature of the nebular gas. The energy cascade is linear from a scale of 9 pc to 1.4 pc.

3. In a H II region experiencing champagne flow, the development of Kelvin-Helmholtz instabilities is a possible source of energy for the development and maintenance of turbulence.

The authors gratefully acknowledge John M. Scalo for his critical reading of an early version of this paper. James Lequeux, Pierre Barge, Serge Pineault, Richard N. Henriksen, and Marshall McCall made helpful comments and suggestions. Carmelle Beaulieu and Guy Plante helped in preparing the manuscript. The National Science and Engineering Research Council of Canada and the Fond FCAC of Québec provided funds to support this research project.

REFERENCES

Arsenault, R., and Roy, J.-R. 1984, *Pub. A.S.P.*, **96**, 496.
Blake, G. M. 1972, *M.N.R.A.S.*, **156**, 67.
Cantwell, B. J. 1981, *Ann. Rev. Fluid. Mech.*, **13**, 457.
Courtès, G. 1955, in *IAU Symposium 2, Gas Dynamics of Cosmic Clouds*, ed. H. C. van de Hulst and J. M. Burgers (Amsterdam: North-Holland), p. 131.
de Vaucouleurs, G. 1979, *Astr. Ap.*, **79**, 274.
Gallagher, J. S., and Hunter, D. A. 1983, *Ap. J.*, **274**, 141.
Garay, G., and Rodríguez, L. F. 1983, *Ap. J.*, **266**, 263.
Henriksen, R. N., Bridle, A. H., and Chan, K. L. 1982, *Ap. J.*, **257**, 63.
Humphreys, R. M. 1978, *Ap. J. Suppl.*, **38**, 309.
Israël, F. P. 1980, *A.J.*, **85**, 1612.
Joncas, G. 1983, Ph.D. thesis, Université Laval.
Joncas, G., and Roy, J.-R. 1984*a*, *Pub. A.S.P.*, **96**, 263.
———. 1984*b*, *Ap. J.*, **283**, 640.
Joncas, G., Roy, J.-R., Dewdney, P., and Higgs, L. H. 1984, in preparation.
Kahn, F. D. 1980, *Astr. Ap.*, **83**, 303.
Kaplan, S. A. 1966, *Interstellar Gas Dynamics*, ed. F. D. Kahn (New York: Pergamon Press).
Kaplan, S. A., and Pikelner, S. B. 1970, *The Interstellar Medium* (Cambridge: Harvard University Press), p. 336.
Kolmogorov, A. N. 1941, *Dokl. Akad. Nauk. SSR*, **30**, 301.
Larson, R. B. 1979, *M.N.R.A.S.*, **186**, 479.
———. 1981, *M.N.R.A.S.*, **194**, 809.
Lazareff, B. 1983, in *Diffuse Matter in Galaxies*, ed. J. Audouze, J. Lequeux, M. Lévy, and A. Vidal-Madjar (Dordrecht: Reidel), p. 141.
Leung, C. M., Kutner, M. L., and Mead, K. N. 1982, *Ap. J.*, **262**, 583.
Lighthill, M. J. 1955, in *IAU Symposium 2, Gas Dynamics of Cosmic Clouds*, ed. H. C. van de Hulst and J. M. Burgers (Amsterdam: North-Holland), p. 121.
Louise, R., and Monnet, G. 1970, *Astr. Ap.*, **8**, 486.
Melnick, J. 1977, *Ap. J.*, **213**, 15.
———. 1978, *Astr. Ap.*, **70**, 157.
Moffat, A. F. J. 1971, *Astr. Ap.*, **13**, 30.
Münch, G. 1958, *Rev. Mod. Phys.*, **30**, 1035.
Myers, P. C. 1983, *Ap. J.*, **270**, 105.
Norman, M. L., Smare, L., Winkler, K.-H. A., and Smith, D. H. 1982, *Astr. Ap.*, **113**, 285.
Pedlar, A. 1980, *M.N.R.A.S.*, **192**, 179.
Rayo, J. F., Peimbert, M., and Torres-Peimbert, S. 1982, *Ap. J.*, **255**, 1.
Rosa, M., and Solf, J. 1984, *Astr. Ap.*, **130**, 29.
Sandford, M. J., II, Whitaker, R. W., and Klein, R. I. 1982, *Ap. J.*, **260**, 183.
Scalo, J. M. 1984, *Ap. J.*, **277**, 556.
Tennekes, H., and Lumley, J. L. 1972, *A First Course in Turbulence* (Cambridge: The MIT Press).
Tenorio-Tagle, G. 1979, *Astr. Ap.*, **71**, 59.
Von Hoerner, S. 1951, *Zs. Ap.*, **30**, 17.
Wilson, O. C., Münch, G., Flather, E. M., and Coffeen, M. F. 1959, *Ap. J. Suppl.*, **4**, 199.

GILLES JONCAS: Observatoire de Marseille, 2 Place Le Verrier, 13248 Marseille, Cedex 4, France

JEAN-RENÉ ROY: Département de physique, Université Laval, Québec, QC G1K 7P4, Canada